Resveratrol Nanocrystal Loaded Orodispersible Films: Formulation Development and In Vitro Characterization

Samet Ozdemir
Istanbul Health and Technology University: Istanbul Saglik ve Teknoloji Universitesi
Burcu Uner
Yeditepe University: Yeditepe Universitesi
Alptug Karakucuk (alptug.karakucuk@ankaramedipol.edu.tr)
Ankara Medipol Universitesi https://orcid.org/0000-0002-9061-2427

Research Article

Keywords: Resveratrol, nanocrystal, bottom-up, orodispersible films, solvent casting

Posted Date: September 14th, 2021

DOI: https://doi.org/10.21203/rs.3.rs-873761/v1

Abstract

Nanocrystals are a feasible system to improve the aqueous solubility of poorly soluble compounds. Orodispersible films (ODFs) offer a rapid release of the drug in the mouth and are preferred for patients with dysphagia or paediatrics. The objective of the current study was to develop resveratrol (RES) nanocrystal-loaded ODFs. RES nanocrystals were prepared by antisolvent precipitation in the existence of Poloxamer 188 as a polymeric stabilizer. Polyvinyl alcohol was used for the preparation of the ODFs by using the solvent casting method. Then, RES nanocrystals were incorporated into the films. Particle size (PS), polydispersity index (PDI), and zeta potential (ZP) values were measured for nanocrystals. ODFs were characterized, and bioadhesion, disintegration, and in vitro release studies were performed. RES nanocrystals were obtained with 631 nm PS, 0.314 PDI and − 14.3 ZP values. Over 90% of RES nanocrystals were loaded in ODFs, which were approximately 75 μm in thickness. The thermal and crystal properties of nanocrystals in ODFs were preserved regarding DSC and FTIR analyses. Homogenous distribution in smooth films was observed on SEM. Mechanical properties and bioadhesion forces were found to be appropriate for ODFs. The disintegration time was found below 30 seconds for nanocrystal loaded films. RES nanocrystal loaded film formulations showed > 85% release in 5 minutes, significantly higher ($p < 0.05$) than those prepared with coarse RES. Novel RES nanocrystal-loaded ODFs can be a promising delivery system for use as an antioxidant with improved patient compliance by increasing solubility and physical stability of RES.

Introduction

Resveratrol (3,4',5-trihydroxy-trans-stilbene, RES) is a non-flavonoid polyphenolic phytoalexin and belongs to the group of stilbenes found in grapes, peanuts, berries, and many natural foods [1]. The chemical structure of RES is responsible for biological activity, which enables the interaction between cellular receptors and enzymes. RES has a potent antioxidant activity by targeting extracellular radical oxygen species when administered orally [2]. RES has many pharmacological activities, including antioxidant, anti-inflammatory, anti-cancer, anti-microbial, anti-hypertensive, cardioprotective, and anti-diabetic, and formulations are being developed by pharmaceutical companies or academic research [3, 4]. RES is practically insoluble in water (0.03–0.05 mg/mL); however, it exhibits high membrane permeability (log P: 3.1) and belongs to the Biopharmaceutical Classification System (BCS) Class II drugs [5]. Due to the very low bioavailability (< 5% of the oral dose is detected in plasma) and fast metabolism, the biological effectiveness of RES has been restricted to use in cosmetics, foods, and drugs [6, 7]. RES has two geometric isomers, *cis*- and *trans*-, trans isomer is the primary, biologically more active, and more stable natural form. However, RES is very sensitive to sunlight or artificial, and natural UV, heat, enzymes, and *cis*-isomerization can occur after light exposure [8, 9].

Nanocrystals, also known as nanosuspensions, are a feasible approach to increase water solubility, drug stability and overcome the limitations of BCS Class II drugs such as *trans*-RES by diminishing the particle size typically between 200–600 nm [10–12]. The primary advantages of nanocrystals are high-drug loading capacity, applicability to various administration routes, ease of scale-up, relatively low-cost

formulation, and production processes [13]. Several commercially available products (Rapamune, Emend, Avinza, Ritalin LA, Tricor) were released regarding formulation development and scale-up success of the system [14].

There are two main approaches to prepare nanocrystal formulations, top-down and bottom-up. In the top-down method, micrometre range drug crystals break up into nanoscale by high-pressure homogenization or wet ball grinding techniques [15]. The bottom-up approaches are solvent evaporation, supercritical fluid, chemical, and anti-solvent precipitation [10]. Among them, with the simplicity and cost-effectiveness benefits, the antisolvent precipitation method is the most common and effective technique to produce nanocrystals [16]. In this method, the drug is dissolved in the organic solvent and added to the antisolvent phase immediately. Thus, the drug particles precipitate under the super-saturated conditions achieved by the solution transfer [17]. Although top-down methods do not require organic solvents and are more beneficial for the industry, they usually need more prolonged formulation and production time. In addition, they consume higher energy resulting in heat and deformation of crystals, making it difficult to process the thermolabile compounds [12]. On the contrary, the bottom-up method has some advantages, such as simple instruments, fewer validation parameters, and lower energy demand [18].

Because of the tendency to reduce the excessive surface energy, nanocrystals in suspension can agglomerate, or Ostwald ripening phenomenon can arise. Surfactants, polymers, or lipids can stabilize the nanocrystal system by generating steric and ionic stabilization [19]. Nanocrystal dispersion can be solidified by lyophilization, spray drying, or fluid bed granulation to improve physical stability and develop solid dosage forms or transformed to semi-solid dosage forms, such as gels or films [16, 20].

Solid dosage forms, especially tablets, have always been the first choice for drug development and administration. However, geriatric and paediatric patients, and those who suffer from swallowing difficulty or vomiting, have the most compliance issues about the proper dosage forms for their needs [21]. Orodispersible films (ODFs) can be advantageous for these patients with rapid disintegration in the mouth, no need for water intake, chew or swallow, and no risk of choking [22]. According to European Pharmacopeia, the definition of ODFs are single or multilayered sheets of suitable materials to be placed in the mouth where they disperse rapidly [23]. ODFs are prepared using methods of solvent casting, hot-melt extrusion, electrospinning, or printing (inkjet, flexographic, and 3D printing) [24]. The solvent casting method is most common to produce ODFs. In this technique, the drug compound is dissolved or dispersed in a polymer solution. If necessary, plasticizers, taste-masking agents, and fillers can be added. After that, the polymer solution is cast with the desired thickness on a flat surface, dried, and films are collected [25]. Nanocrystal-loaded ODFs can be an innovative drug delivery system for individual patient needs with enhanced solubility and stability properties of BCS Class II drugs.

The objective of the present study was to develop RES nanocrystals-loaded ODFs. Nanocrystals were prepared by the anti-solvent precipitation method. After obtaining nanoscale range particle size, RES nanocrystals were loaded into ODFs to develop easy-to-use patches and hence improve patient

compliance. The characterization, disintegration, and in vitro release studies were conducted to evaluate the nanocrystal-loaded film formulations.

Materials And Methods

Materials

Resveratrol and Poloxamer 188 were purchased from Sigma-Aldrich (Germany). Polyvinyl alcohol (PVA) (6000 kDa) was obtained from EastChem (China). Acetone and glycerin were purchased from Merck-Millipore (USA). HPLC eluent acetonitrile (> 99.9%) was obtained from Sigma-Aldrich (Germany), and simulated salivary fluid was purchased from Biochemazone (Canada).

Preparation of RES nanocrystals

RES nanocrystal was prepared with the anti-precipitation method. Firstly, the organic solvent was selected. For this purpose, RES was dissolved in ethanol, methanol, and acetone in increasing proportions. Then, the solutions were examined visually, and according to gravimetric solubility analysis, RES in acetone showed the highest solubility; therefore, it was selected as the organic solvent.

For the preparation of the anti-solvent phase, Poloxamer 188 as a stabilizer was dissolved in distilled water. Different Poloxamer 188 amounts (1%, 2%, 3% w/w) were dissolved in distilled water. It was observed particle agglomeration with 1% concentration. Besides, the RES particles were not precipitated with 3% of concentration. Therefore, 2% concentration was found optimum for the stabilizer solution. After that, the organic phase was dropped into the stabilizer solution (solvent: antisolvent 3:20) at an injection rate of 1 mL/min using a magnetic stirrer at 300 rpm. Stirring was continued for 15 minutes, and nano-precipitated RES was obtained. The homogenization process was performed either ultraturrax at 20 000 rpm for 5 minutes or ultrasonic probe with 75% amplitude (amp) for 5 minutes (Table 1). Particle size (PS), polydispersity index (PI), and zeta potential (ZP) values were measured to characterize the nanocrystals.

Table 1
The formulation composition of nanocrystals

Formulation code	Solvent: antisolvent	Polymer (w/w %)	RES (mg)	Ultraturrax (min, rpm)	Ultrasonic probe (min, amp%)	Stirring (rpm, min)
F1	3:20	2	100	-	-	300, 15
F2	3:20	2	100	-	5, 75	300, 15
F3	3:20	2	100	5, 20.000	-	300, 15
F4	3:20	2	200	-	-	300, 15
F5	3:20	2	200	-	5, 75	300, 15
F6	3:20	2	200	5, 20.000	-	300, 15

Preparation of RES nanocrystals loaded ODFs

The ODFs of RES nanocrystals were prepared using the solvent casting method. For this purpose, PVA (8% w/w) was dissolved in distilled water. The RES nanocrystals were kept for one day before adding them to the polymer solution. Then, RES nanocrystals and PVA solution (1:1) was added in a 6 cm radius polystyrene petri dish (Isolab, Germany) (4 g) without (F7) or with glycerin (F8) as a plasticizer (5% w/w) and dried at 45^{o}C in an oven. The similar cast films were also prepared with coarse RES particles (F9, F10) to compare the results with nanocrystal loaded films (Table 2).

Table 2
The formulation composition of the ODFs

Formulation code	Polymer (w/w %)	Glycerin (w/w %)	RES nanocrystal (w/w %)	RES coarse suspension (w/w%)
F7	50	-	50	-
F8	49	1	50	-
F9	50	-	-	50
F10	49	1	-	50

Characterization studies

Particle size (PS), polydispersity index (PDI), and zeta potential (ZP)

PS, PI, and ZP values of precipitated RES nanocrystals were measured using Malvern ZetaSizer (Malvern Instruments, UK). 25 µL of RES nanocrystals were dropped in a measurement cuvette immediately after collecting them from the magnetic stirrer, after the ultraturrax process or after the ultrasonic probe. The nanocrystal was diluted up to 5 mL of distilled water, and measurements were recorded as average ± S.D.

Drug content

The drug content in film formulations was analyzed by UV spectrophotometric method. A filmstrip of about 1x1 cm^2 area was dissolved in 10 mL of methanol at room temperature. The solution was filtered from a 0.45 µm membrane filter. The filtrate was analyzed at 306 nm [26].

Film thickness

The thickness of the ODFs was measured using digital Vernier Calipers (Mitutoyo®, Japan, 0.01 mm sensitivity from three different places of the film, and the average ± S.D. was calculated.

Weight variation

For the measurement of weight variation, 25 cm^2 films were cut at five different places in the cast film. Then, the weight of each filmstrip was taken, and the weight variation was calculated [26, 27].

Surface pH

The surface pH of the films was measured after the films were placed in contact with the electrode of a pH meter (Hanna® Instruments, HI-5522-02, Germany). Equilibration for 30 s was allowed to determine the surface pH. Results were collected three times for each formulation, and the average ± S.D. was calculated [28].

Differential scanning calorimetry (DSC)

DSC studies were conducted to determine the melting points of the formulations after the nanocrystal, and ODFs preparation process (Setaram, DSC131, France). 5 mg of the samples were weighed placed in sealed aluminium pans, crimped and sealed. The temperature was elevated up to 300 ^oC starting from 25 ^oC under cover of nitrogen gas (50 mL/s) with a heating rate of 10 ^oC/min.

Scanning electron microscopy (SEM)

Morphological characterization of cast films was achieved by using an SEM (Zeiss EVO 10, USA). The study was conducted with an accelerating voltage of 15.00 kV. Surfaces of the prepared samples were coated with gold and palladium using sputter (LEICA EM ACE200, Leica Microsystems, Germany) at 3 kV for 60 s. SEM images were captured with different magnifications under high vacuum conditions.

Fourier-transform infrared spectroscopy (FTIR)

The spectra of cast films were obtained in the wavenumber range of 650–4000 cm^{-1} using an FTIR (NICOLET iS50, Thermo Scientific, USA). The inserts were gently cut with a scalpel blade, and the

samples were directly put over the crystal of the equipment. Multiple scans were applied for each sample, and the force over the samples was adjusted to achieve transmittance results.

Mechanical properties, swelling index, and bioadhesion studies

Mechanical properties, such as tensile strength, Young's modulus, and elongation at break of the films were measured using a TA-XT texture analyzer (Stable Micro Systems, UK, the range was 0-100 N). The initial grip distance was constant, 30 mm, and the rate of the grip separation was 100 $mm.min^{-1}$. All samples were stabilized in the given conditions overnight and cut into 15 mm wide with a lab film cutter. Each study was performed for six replicates. The thicknesses of each sample were measured with a digital calliper from three different points. The average thickness was used for the calculations [29].

The films' swelling index studies were conducted in the simulated salivary fluid (Biochemazone®, Canada) at pH 6.8. The film sample (surface area 1 cm^2) was weighed and placed in a pre-weighed stainless-steel basket (Pharma Test, Germany) of approximately 100-µm mesh. The basket containing the film sample was submerged into 50 mL of simulated salivary fluid in a beaker. At a definite time interval (10 s), the stainless-steel basket was removed, excess moisture removed by carefully wiping with absorbent tissue, and re-weighed. Increasing the weight of the films was determined at each time interval until a constant weight was observed. The degree of swelling was calculated using the following equation (Eq. 1) [30];

$$Swellingindex = (wt - wo)/wo$$ Eq. 1.

Where; wt is the weight of film at time t, and wo is the weight of film at time zero.

Work of Bioadhesion values was measured using Texture Analyzer with different settings and assembling modifications (TA-XT plus, Stable Microsystems, UK; maximum load 50 kg). The sample holder was rod-like with a diameter of 5 mm. A double-faced adhesive tape was fixed on the surface of the sample holder, and the film formulations were set on the other face of the adhesive tape. A disc with a 35-mm diameter was fixed on the bottom part of the tester, and simulated salivary fluid was spread on it. The rod-like sample holder was moved downward and pressed to the saline-covered bottom disc with 30 ± 0.1 N for 30 s. The force-time curve followed this steady-state part. After that, the sample holder was moved upwards, and the force was decreased until the sample started to separate from saline, which can be seen as a well-defined peak in the force-time curve. The peak maximum illustrated the bioadhesive force.

In vitro disintegration time and in vitro release studies

In vitro disintegration time was measured by the Petri dish method. The film formulations were dropped in a culture dish of 6 cm in diameter, containing 10 mL of simulated salivary fluid. The mean in vitro dispersion time ± S.D. was determined.

The in vitro release studies of RES nanocrystal loaded films were tested using USP dissolution tester Apparatus II (Pharma Test, Germany). The cast films were cut into 1 cm^2 pieces, which were equivalent to 7 mg of RES. The paddles were rotated at 50 rpm in 900 mL of simulated salivary fluid (Biochemazone®, Canada, pH 6.8). The temperature of the water bath was kept at 37 ^oC ± 0.5 ^oC. Aliquots of 5 mL were withdrawn from the dissolution medium at pre-determined time intervals (1, 3, 5, 7, 10, 15, 20, 25, and 30 min) and then replaced with a fresh medium to maintain the sink conditions. The samples were filtered through a Millipore filter (0.45 µm), and RES content was determined using an HPLC spectrophotometer.

HPLC method

The HPLC method was validated as described by Singh and Pai [31]. Reversed-phase isocratic conditions were performed using Agilent 1100, USA. The separation was achieved by the C18 column (Accucore™ XL Thermo Scientific™ 250x2.1 mm, 4 µm) with UV detection at 306 nm. The optimized mobile phase consisted of a mixture of methanol: 10 mM potassium dihydrogen phosphate buffer (pH 6.8): acetonitrile (63: 30: 7, v/v/v) at a flow rate of 1 mL/min.

Statistical analysis

The software package Prism v. 5.04 (GraphPad Software Inc., La Jolla, CA, USA) was used to analyze variance (ANOVA) to detect differences among the mean values of responses and for the curve fitting with performing Tukey HSD post-hoc test. Data were presented as mean ± standard deviation (S.D.), and a value of $p < 0.05$ was taken as the level of significance.

Results And Discussion

Preparation and evaluation of RES nanocrystals

This research focused on preparing RES nanocrystals using a bottom-up approach and then incorporating nanocrystals into ODFs. It might be a beneficial formulation development method for ODFs using other drug delivery carriers, such as nanocrystals, solid lipid microparticles or self-emulsifying systems [32]. Preparation of ODFs with nanocrystals provide transforming nanocrystals into a solid dosage form to improve physical stability and enhance aqueous solubility and hence oral bioavailability of poorly soluble drugs [33].

To produce RES nanocrystals, one of the bottom-up approaches, the anti-precipitation method, was used. In general, the critical formulation parameters for this method are solvent: antisolvent ratio, polymer type and concentration, drug amount, the injection rate of the solvent to the antisolvent, stirring time and speed. Nanocrystals are typically systems with particle sizes between 100–1000 nm. PDI values between 0.1–0.4 are desired to avoid Ostwald ripening. Also, ZP is crucial for the system's physical stability, which is desired to be far from zero. After the nanoprecipitation, the combined methods, such as wet grinding, high pressure homogenization, can be used. In this study, the homogenization process was performed after nanoprecipitation using ultraturrax or ultrasonic probe. After the formulation and process

parameters were optimized, critical control parameters PS, PDI and ZP were measured. The PS of RES nanocrystals were found at 631 nm after the ultraturrax process. PDI and ZP values were achieved to 0.314 and − 14.3 mV, respectively (Table 3). The PS, PDI and ZP values were not changed after one day of storage and in ODFs.

Table 3
Particle size, polydispersity index, and zeta potentials of nanocrystal formulations

Formulation code	PS (nm)			PDI			ZP (mV)		
F1	7028.6	±	2.29	0.997	±	0.02	1.57	±	0.07
F2	2029.5	±	1.46	0.611	±	0.07	0.947	±	0.05
F3	834.8	±	1.87	0.516	±	0.05	-5.48	±	0.05
F4	6002.9	±	3.19	0.818	±	0.04	0.017	±	0.01
F5	1983.5	±	2.04	0.604	±	0.05	-3.26	±	0.04
F6	631.0	±	2.16	0.314	±	0.02	-14.3	±	0.02

Characterization studies of ODFs

After loading nanocrystals and coarse powder of RES, ODFs were prepared by solvent casting method. It was challenging to remove glycerin-free film formulations from Petri dishes. On the other hand, formulations with glycerin were removed from Petri easily. Also, adding glycerin as a plasticizer provided brighter and softer ODFs, and homogeneous distribution of RES nanocrystals was observed (Fig. 1). Finally, characterization studies were performed for nanocrystal, and coarse powder loaded ODFs.

a b

Drug content

The RES content in film formulations was over 93% for nanocrystal and coarse powder loaded films (Table 4). The higher drug content in the ODF preparations exhibited the uniform dispersion of RES in the film matrix; thus, an accurate dose delivery can be achieved. Similar results have been reported using different polymers, or polymer combinations (cellulose derivatives and pullulan) indicate drug contents in a range of 90–99% [34, 35]. Thus, the outcomes of the drug content study were compatible with the literature data.

Weight variation

The weight of ODFs was found in the range of 11–15 mg (Table 4). The standard deviation of all the samples was very low; thus, the ODF preparations were uniform in weight. Therefore, the accuracy of the dose can achieve by a uniform weight distribution with high drug content.

Film thickness

The thickness values of the ODFs were found approximately 75 μm (Table 4). Uniformity of the film thickness is a critical quality attribute to provide homogenous distribution of the dose. Furthermore, in ideal conditions, ODFs should exert acceptable mechanical properties such as flexibility and physical durability. The typical film thickness was reported in a range of 12–100 μm [36]. The thickness of ODFs is dependent mainly on the polymer concentration in cases of lab-scale production. Because the polymeric mixture is generally poured into a petri dish, the thickness of the film is directly related proportionally to the polymer concentration. Similarly, CMC was used as a film-forming polymer in a study, and the thickness was directly affected by the polymer concentration [37]. In this case, the concentration of the polymer was selected by considering the film thickness around 75 μm.

Surface pH

The pH values of the ODFs were found between 6.8–7.12 (Table 4). The saliva pH is reported in the range of 5.8–8.4, so surface pH for the ODFs should be chosen close to neutral pH [38]. The acceptance of the formulations by the patients also depends on the pH due to possible irritation risks.

Table 4
Weight variation, thickness, and surface pH of the cast film formulations

Formulation	Drug content (%)	Weigh variation (mg)	Thickness (μm)	Surface pH
F7	93.81 ± 0.402	0.15 ± 0.028	73.79 ± 0.331	6.83 ± 0.013
F8	94.26 ± 0.244	0.12 ± 0.022	74.12 ± 0.162	7.01 ± 0.028
F9	96.47 ± 0.328	0.14 ± 0.015	74.53 ± 0.196	6.99 ± 0.010
F10	94.58 ± 0.706	0.11 ± 0.023	74.67 ± 0.304	7.12 ± 0.034

Differential scanning calorimetry (DSC)

Determination of solid-state interactions and melting points were determined using DSC to assess the effect of both without RES nanocrystals and RES nanocrystals on the thermal stability of the PVA matrix. For coarse resveratrol, the melting process occurred with a maximum peak at 235.53°C (Fig. 2). This result was compatible with literature data [39]. The endothermic peak of RES completely disappeared in film formulations that demonstrate PVA dissolved RES after it melts. During the heating scan, the F7 glass transition (T*g*) temperature occurred at 81.4°C. Concerning the F9 formulation, by adding the coarse RES instead of the nanocrystal, T*g* gradually increased to an average value of 118.7°C. Also, an increase was observed with F10 in comparison with RES nanocrystal loaded ODFs. In both of the thermograms of the F8 and F10 formulations, it was observed that the melting point started earlier than the F7 and F9 formulations due to the glycerin content [40].

Scanning electron microscopy (SEM)

SEM is the most convenient visual technique to prove particles' mean size and surface morphology. The low resolution of the photograph, the SEM image of F7 showed the random distribution of the individual RES nanocrystals in the film. The irradiation has a relatively rough surface and microporous structure, which may be due to the partial degradation of PVA by the exposure of RES nanocrystals to irradiation [41]. It was evident that the surface morphology of F7 and F9 films were plane and smooth, but the F8 and F10 formulations, which contained glycerin, showed a surface with uneven morphology and cracks (Fig. 3). SEM images indicated that the droplet size of RES nanocrystals was homogenous. Moreover, SEM analysis supported data obtained from size measurements by DLS.

Fourier-transform infrared spectroscopy (FTIR)

ATR-FTIR analysis was used to test the changes in the chemical composition of RES and film formulations, as shown in Fig. 4. A sharper peak was observed at between 1200–1300 cm^{-1} of film formulations, and other sharper peaks were distributed at between 1200 – 1100 cm^{-1}, 1400 – 1300 cm^{-1}, 1600 – 1500 cm^{-1}, which were ascribed to the oxygen-containing groups, such as s aldehyde C = O stretch, Carboxylic acid-COOH stretch, and aldehyde/ketone C-O peaks of PVA [42]. Pure resveratrol showed a typical trans olefinic band between 1000 – 900 cm^{-1} and the narrow O-H stretching at 3300 cm^{-1}. Three characteristic intense bands were between 1400 – 1300 cm^{-1}, 1600 – 1500 $cm^{-1,}$ and 1700 – 1600 $cm^{-1,}$ corresponding to C–O stretching, C–C olefinic stretching, and C–C aromatic double-bond stretching, respectively. For F9 and F10 formulation, remarkable shifting of C-O-C and C = O absorption band of RES from between 1600 – 1500 cm^{-1} from 1700 – 1600 cm^{-1} respectively, indicating interference at the polar head of coarse RES [43].

Mechanical properties, swelling index, and bioadhesion studies

Mechanical properties of the ODFs, including bioadhesive force, tensile strength, Young's modulus, and elongation at break, are presented in Table 5. The mucoadhesive properties of films make them attach to the tissue interface, enhancing the efficiency of local therapy [44]. The adhesive properties in vitro of films were evaluated. Film formulations adhered between two smooth glass surfaces, and the corresponding maximum load was 40, 50, and 50 g, respectively. Coarse RES powder loaded films improved the adhesive strength in comparison with RES nanocrystals loaded ODFs. In addition, it can be said for both F8 and F10 formulations that the addition of glycerin also increases bioadhesion. Similar results are shown in the literature [45]. Tensile strength is explained as the maximum load force used to break the film. Hard and brittle substrates demonstrate very high mechanical resistance [46].

Elongation at break and tensile strength of F7 was found 62.9% and 9.14 MPa, respectively. On the contrary, using coarse powder of RES was enhanced elongation at break and tensile strength to 73.06% and 10.88 MPa, respectively. This can be explained as the coarse drug molecules, which dispersed more heterogeneously than nanocrystals, were interposed the linkages of the polymers. Regarding durability

enhancement, both the values were decreased by adding glycerin to the film formulations, either coarse powder or nanocrystal [47].

In the pre-formulation part, removing the cast films without plasticizer from the moulds was challenging because of their brittleness. Thus, a plasticizer (glycerin) was added to the polymeric dispersions to improve mechanical properties. Young's modulus is associated with film stiffness and the capacity to undergo elastic deformation under applied stress [46]. The addition of the coarse RES particles instead of nanocrystals also increased Young's Module.

Film formulation results showed that folding endurance was in the range of 201 ± 0.542 to 217 ± 0.833 (Table 5). Folding endurance decreased using coarse powder of RES without glycerin. Similarly, the use of coarse powder in films prepared with glycerin caused a decrease in folding endurance. The folding endurance was obtained optimum with formulation F8 (217 ± 0.833) due to the presence of nanocrystal and glycerin [47, 48]. Finally, the data obtained from the mechanical tests were correlated with each other.

Table 5
Mechanical properties and bioadhesive forces of the film formulations

Formulation Code	Bioadhesive Force (mJ/cm^2)	Tensile Strength (Hardness) (MPa)	Young's Module (MPa)	Elongation at Break (%)	Folding Endurance
F7	0.353 ± 0.013	9.14 ± 0.018	13.87 ± 0.108	62.33 ± 0.042	205 ± 0.511
F8	0.388 ± 0.027	8.96 ± 0.047	13.11 ± 0.233	60.04 ± 0.062	217 ± 0.833
F9	0.496 ± 0.082	10.88 ± 0.014	16.42 ± 0.120	73.06 ± 0.021	201 ± 0.542
F10	0.511 ± 0.077	10.14 ± 0.023	16.04 ± 0.252	70.06 ± 0.054	214 ± 0.408

A swelling test was performed *in situ* by introducing films with simulated salivary fluid (pH 6.8) in a pre-weighed stainless-steel basket. The films remained stable throughout all measurements. The surface of the films participated in saliva over the 60 seconds of the swelling period. The blend films' swelling index (SI) at 10 to 60 seconds varied from 3.24 to 5.29, as shown in Table 6. The SI of all film formulations increased rapidly during the first 10 seconds and reached a swollen equilibrium by 60 seconds. The decrease in SI at 30 and 40 seconds of the films indicated erosion of the films. As seen in F8 and F10, adding glycerin as a plasticizing agent increases SI [49]; also indicate that the hydration rate and water uptake of coarse RES films were faster than nanocrystal films. This proves that the film formulation containing the nanocrystal contributes to swelling in a more controlled and rapid manner [30, 50].

Table 6
Swelling index values of film formulations (mean ± S.D., n = 6)

Time (sec)	F7			F8			F9			F10		
10	3.26	±	0.151	3.92	±	0.205	3.29	±	0.274	3.99	±	0.233
20	4.12	±	0.226	4.53	±	0.114	4.19	±	0.229	4.56	±	0.182
30	5.22	±	0.184	5.48	±	0.188	5.27	±	0.107	5.49	±	0.109
40	5.24	±	0.122	5.51	±	0.126	5.31	±	0.143	5.56	±	0.275
50	5.28	±	0.109	5.53	±	0.117	5.32	±	0.119	5.57	±	0.121
60	5.28	±	0.238	5.54	±	0.255	5.32	±	0.152	5.59	±	0.086

In vitro disintegration time and release studies

Ideally, an ODFs should be mechanically flexible with acceptable taste and should provide a rapid release. Conceptually, it was stated that the disintegration time of an ODFs should be as short as possible [36]. However, there was an inverse relation reported between mechanical properties and disintegration time [36, 51]. According to the outcomes (disintegration times are shown in Table 7), the disintegration values were less than 60 sec. Nonetheless, nanocrystal loaded cast films showed faster disintegration in comparison with coarse particles. In European pharmacopoeia, less than 3 min is the required disintegration time for solid oromucosal formulations. Food and Drug Administration (FDA) specifies a disintegration time of less than 1 min for this kind of formulation [51, 52]. In this context, all the designed formulations can be accepted as immediate acting dosage forms. In a study, a cellulose derivative (hydroxypropyl methylcellulose) was selected as a film-forming polymer, and the disintegration time was found to be in the range of 5–30 seconds [34]. Another study was stated that the increased polymer concentration (hydroxymethyl cellulose) decreases the disintegration rate in ODFs, but the disintegration time was still in the 10–60 seconds range [53].

Moreover, alternative polymers rather than cellulose derivatives can be used as film-forming agents in ODFs. For example, in a study, an alternative polymer named pullulan was used to form ODFs. In that study, two different disintegration methods were selected. As a result, it was found to be similar disintegration behaviours (drop method: 28.8 sec. and petri dish method 51.3 seconds) compared to previous studies [38].

Table 7
Disintegration time of the film formulations (mean ± S.D., n = 6)

Formulation	Disintegration time (s)		
F7	28.81	±	0.47
F8	33.48	±	0.23
F9	30.43	±	0.41
F10	34.11	±	0.59

The dissolution profile of a dosage form is crucial for predicting the in vivo action of an active pharmaceutical agent. Conventionally, the release studies are performed under sink conditions. European pharmacopoeia defines the sink condition as a volume of dissolution medium that is at least three to ten times the saturation volume. Thus, resveratrol solubility was detected from the literature data in a range of 0.05 mg/mL (water) to 374 mg/mL (polyethylene glycol 400) in various solvents [54]. After that, the dissolution medium volume and content were determined, and other parameters were selected by considering the body's physiological conditions.

Considering the testing time and cumulative drug release, there was no specific value reported for the ODFs. However, a standard testing period was reported between 30 and 60 minutes, as specified in individual monographs, with cumulative drug release not less than 60% in 30 minutes or 80% in 60 minutes for orally disintegrating tablets [55]. Therefore, the cumulative drug release was investigated based on this data. The RES nanocrystal was released in film formulations approximately 100% in 25 minutes (Fig. 5). RES nanocrystal loaded film formulations showed > 85% release in 5 minutes which was significantly higher ($p < 0.05$) than the films prepared with coarse RES (69.33% and 75.38% for coarse RES films with glycerin and without glycerin, respectively)

After determining release conditions, calculation of the release kinetics by testing different mathematical models illuminates the dissolution profile. Thus, zero-order, first-order, Higuchi, Korsmeyer-Peppas and Hixon-Crowell mathematical models [56] were investigated (Table 8). The mathematical model was chosen by using the correlation coefficient of the related model. As can be seen from the outcomes, coarse suspension incorporated ODFs were best fitted to the Higuchi release model. While RES nanocrystal incorporated ODFs were best fitted to the Korsmeyer-Peppas release model.

Table 8
Mathematical models of release kinetics of ODFs.

	Zero-Order (R2)	First-Order (R2)	Higuchi (R2)	Korsmeyer-Peppas (R2 (n))	Hixson-Crowell (R2)
F7	0.8174	0.6893	0.9417	0.9758 (0.504)	0.9624
F8	0.8106	0.6974	0.9396	0.9847 (0.5117)	0.9609
F9	0.7903	0.7138	0.9519	0.9229 (0.328)	0.9471
F10	0.8006	0.7052	0.9601	0.9253 (0.385)	0.9523

Higuchi type mathematical model describes drug dissolution from matrix systems. This model was reported in many cases and is also transposable for other types of dosage forms [56]. The coarse RES suspension loaded ODFs had high correlation coefficients (F9: 0.9519, F10: 0.9601) and was fitted to the Higuchi model. In this case, ODFs are considered heterogeneous and planar matrices with two regions for the drug release. The inner region includes undissolved drug particles, and the outer region has all the dissolved drug products. Moreover, a concentration gradient is defined, which controls the release rate, according to Fick's law. Although the comments explain this release mechanism, the research shows that the Higuchi model continuously evolves [57].

Korsmeyer-Peppas mathematical model was described for specifically polymeric systems. This model is alternatively called "power law" due to its n value as the release exponent. The "n" predicts the release mechanism of a drug as an example; $0.45 \leq n$ corresponds to Fickian diffusion mechanism, $0.45 < n < 0.89$ to non-Fickian transport, $n = 0.89$ to Case II transport, and $n > 0.89$ to super case II transport [58]. According to the data obtained from the release studies, nanocrystal loaded ODFs have high correlation coefficients (F7; 0,9758, F8; 0,9847) with have n value around 0.5. According to the literature data, these findings best fit the anomalous transport mechanism from the planar matrices [56]. In this case, the "planar matrices" represents the nanocrystal loaded ODFs.

Conclusions

Although approved ODFs are bioequivalent to lyophilizates or immediate-release tablets, substitution is not allowed. Regulatory agencies seem to accept them as a different dosage form, taking the compliance aspect into account. Substitution of ODFs with an immediate-release tablet would lead to enormous problems for patients with swallowing difficulties while substituting an immediate-release tablet with an ODFs is less critical. The magnitude of variants of ODFs technology and the advantages over conventional dosage forms promise more applications and more marketed products with ODFs in the near future. In the present study, ODFs loaded with resveratrol nanocrystals were successfully developed. Desired physical, mechanical, and bioadhesive properties were obtained for the films. Nanocrystals in film formulations showed more rapid disintegration and also quick release. Novel resveratrol nanocrystal-

loaded film formulations can be promising for antioxidant ODFs by increasing the solubility and physical stability of resveratrol.

Declarations

Acknowledgements

The authors would like to thank Prof. Meric KOKSAL AKKOC for providing the facilities to accomplish this study.

Authors' contribution Conception: AK, SO; Design: AK, SO; Supervising: AK; Resources: BU, SO; Materials: BU, SO; Data collection; AK, BU.; Interpretation: AK, BU, SO; Literature search: AK, BU, SO; Writing manuscript: AK, BU, SO; Critical review: AK, SO.

Availability of data and materials

All data obtained during this study are available from the corresponding author on reasonable request.

Funding Not applicable.

Ethics approval and consent to participate Not applicable.

Consent for publication Not applicable.

Competing interests The authors declare that there is no conflict of interest.

References

1. Pujara N, Jambhrunkar S, Wong KY, McGuckin M, Popat A. Enhanced colloidal stability, solubility and rapid dissolution of resveratrol by nanocomplexation with soy protein isolate. J Colloid Interface Sci [Internet]. Elsevier Inc.; 2017;488:303–8. Available from: http://dx.doi.org/10.1016/j.jcis.2016.11.015.
2. Santos AC, Pereira I, Pereira-Silva M, Ferreira L, Caldas M, Collado-González M, et al. Nanotechnology-based formulations for resveratrol delivery: Effects on resveratrol in vivo bioavailability and bioactivity. Colloids Surfaces B Biointerfaces. 2019;180:127–40.
3. Tsai HY, Ho CT, Chen YK. Biological actions and molecular effects of resveratrol, pterostilbene, and 3'-hydroxypterostilbene. J Food Drug Anal [Internet]. Elsevier Ltd; 2017;25:134–47. Available from: http://dx.doi.org/10.1016/j.jfda.2016.07.004.
4. Vasconcelos T, Araújo F, Lopes C, Loureiro A, das Neves J, Marques S, et al. Multicomponent self nano emulsifying delivery systems of resveratrol with enhanced pharmacokinetics profile. Eur J Pharm Sci. 2019;137:105011.
5. Amri A, Chaumeil JC, Sfar S, Charrueau C. Administration of resveratrol: What formulation solutions to bioavailability limitations? J Control Release [Internet]. Elsevier B.V.; 2012;158:182–93. Available

from: http://dx.doi.org/10.1016/j.jconrel.2011.09.083.
6. Wu PS, Li YS, Kuo YC, Tsai SJJ, Lin CC. Preparation and evaluation of novel transfersomes combined with the natural antioxidant resveratrol. Molecules. 2019;24:1–12.
7. Oh WY, Shahidi F. Lipophilization of resveratrol and effects on antioxidant activities. J Agric Food Chem. 2017;65:8617–25.
8. Delmas D, Aires V, Limagne E, Dutartre P, Mazué F, Ghiringhelli F, et al. Transport, stability, and biological activity of resveratrol. Ann N Y Acad Sci. 2011;1215:48–59.
9. Ahmad M, Gani A. Development of novel functional snacks containing nano-encapsulated resveratrol with anti-diabetic, anti-obesity and antioxidant properties. Food Chem [Internet]. Elsevier Ltd; 2021;352:129323. Available from: https://doi.org/10.1016/j.foodchem.2021.129323.
10. Ha ES, Kuk DH, Kim JS, Kim MS. Solubility of trans-resveratrol in Transcutol HP + water mixtures at different temperatures and its application to fabrication of nanosuspensions. J Mol Liq [Internet]. Elsevier B.V.; 2019;281:344–51. Available from: https://doi.org/10.1016/j.molliq.2019.02.104.
11. Keck CM, Müller RH. Drug nanocrystals of poorly soluble drugs produced by high pressure homogenisation. Eur J Pharm Biopharm. 2006;62:3–16.
12. dos Santos AM, Carvalho FC, Teixeira DA, Azevedo DL, de Barros WM, Gremião MPD. Computational and experimental approaches for development of methotrexate nanosuspensions by bottom-up nanoprecipitation. Int J Pharm. 2017;524:330–8.
13. Wang H, Xiao Y, Wang H, Sang Z, Han X, Ren S, et al. Development of daidzein nanosuspensions: Preparation, characterization, in vitro evaluation, and pharmacokinetic analysis. Int J Pharm Elsevier. 2019;566:67–76.
14. Anup N, Thakkar S, Misra M. Formulation of olanzapine nanosuspension based orally disintegrating tablets (ODT); comparative evaluation of lyophilization and electrospraying process as solidification techniques. Adv Powder Technol [Internet]. Society of Powder Technology Japan; 2018;29:1913–24. Available from: https://doi.org/10.1016/j.apt.2018.05.003.
15. Karakucuk A, Celebi N. Investigation of formulation and process parameters of wet media milling method to develop etodolac nanosuspensions. Pharm Res. 2020;37:1–18.
16. Alshweiat A, Katona G, Csóka I, Ambrus R. Design and characterization of loratadine nanosuspension prepared by ultrasonic-assisted precipitation. Eur J Pharm Sci [Internet]. Elsevier; 2018;122:94–104. Available from: https://doi.org/10.1016/j.ejps.2018.06.010.
17. Zhou Y, Fang Q, Niu B, Wu B, Zhao Y, Quan G, et al. Comparative studies on amphotericin B nanosuspensions prepared by a high pressure homogenization method and an antisolvent precipitation method. Colloids Surfaces B Biointerfaces [Internet]. Elsevier; 2018;172:372–9. Available from: https://doi.org/10.1016/j.colsurfb.2018.08.016.
18. Zhao J, Wang Y, Ma Y, Liu Y, Yan B, Wang L. Smart nanocarrier based on PEGylated hyaluronic acid for deacetyl mycoepoxydience: High stability with enhanced bioavailability and efficiency. Carbohydr Polym [Internet]. Elsevier; 2019;203:356–68. Available from: https://doi.org/10.1016/j.carbpol.2018.09.071.

19. Kumar A, Hodnett BK, Hudson S, Davern P. Modification of the zeta potential of montmorillonite to achieve high active pharmaceutical ingredient nanoparticle loading and stabilization with optimum dissolution properties. Colloids Surfaces B Biointerfaces [Internet]. Elsevier; 2020;193:111120. Available from: https://doi.org/10.1016/j.colsurfb.2020.111120.
20. Sahnen F, Kamps JP, Langer K. Conversion of indomethacin nanosuspensions into solid dosage forms via fluid bed granulation and compaction. Eur J Pharm Biopharm [Internet]. Elsevier; 2020;154:89–97. Available from: https://doi.org/10.1016/j.ejpb.2020.06.020.
21. Yafout M, Elhorr H, Ousaid A, Otmani IS, El, Khayati Y. Orodispersible Films as a Solution to Drug Acceptability Issues: A Short Review. Asian J Res Med Pharm Sci. 2021;10:36–41.
22. Wang B, Yang L, Wang B, Luo C, Wang Y, Wang H, et al. Development, In Vitro and Vivo Evaluation of Racecadotril Orodispersible Films for Pediatric Use. AAPS PharmSciTech. AAPS PharmSciTech; 2021;22:p. 15.
23. El-Bary AA, Al Sharabi I, Haza'a BS. Effect of casting solvent, film-forming agent and solubilizer on orodispersible films of a polymorphic poorly soluble drug: an in vitro/in silico study. Drug Dev Ind Pharm [Internet]. Taylor & Francis; 2019;45:1751–69. Available from: https://doi.org/10.1080/03639045.2019.1656733.
24. Łyszczarz E, Hofmanová J, Szafraniec-Szczęsny J, Jachowicz R. Orodispersible films containing ball milled aripiprazole-poloxamer®407 solid dispersions. Int J Pharm. 2020;575.
25. Thabet Y, Breitkreutz J. Orodispersible films: Product transfer from lab-scale to continuous manufacturing. Int J Pharm [Internet]. Elsevier; 2018;535:285–92. Available from: https://doi.org/10.1016/j.ijpharm.2017.11.021.
26. Ahmed MG, Harish NM, Charyulu RN, Prabhu P. Formulation of chitosan-based ciprofloxacin and diclofenac film for periodontitis therapy. Trop J Pharm Res. 2009;8:33–41.
27. Semalty A, Semalty M, Nautiyal U. Formulation and evaluation of mucoadhesive buccal films of enalapril maleate. Indian J Pharm Sci [Internet]. Medknow Publications; 2010;72:571–5. Available from: https://pubmed.ncbi.nlm.nih.gov/21694987.
28. Senthilkumar K, Vijaya C. Formulation Development of Mouth Dissolving Film of Etoricoxib for Pain Management. Adv Pharm. 2015;2015:1–11.
29. Vargas ALM, de Araújo Ribeiro F, Hübler R. Changes in the Young Modulus of hafnium oxide thin films. Nucl Instruments Methods Phys Res Sect B Beam Interact with Mater Atoms [Internet]. 2015;365:362–6. Available from: https://www.sciencedirect.com/science/article/pii/S0168583X15006746.
30. Kraisit P, Limmatvapirat S, Luangtana-Anan M, Sriamornsak P. Buccal administration of mucoadhesive blend films saturated with propranolol loaded nanoparticles. Asian J Pharm Sci [Internet]. 2018;13:34–43. Available from: https://www.sciencedirect.com/science/article/pii/S1818087617304051.
31. Singh G, Pai RS. A Rapid Reversed-Phase HPLC Method for Analysis of Trans -Resveratrol in PLGA Nanoparticulate Formulation. ISRN Chromatogr. 2014;2014:1–6.

32. Musazzi UM, Khalid GM, Selmin F, Minghetti P, Cilurzo F. Trends in the production methods of orodispersible films. Int J Pharm. 2020;576.
33. Shen B, De, Shen CY, Yuan XD, Bai JX, Lv QY, Xu H, et al. Development and characterization of an orodispersible film containing drug nanoparticles. Eur J Pharm Biopharm. 2013;85:1348–56.
34. Rençber S, Karavana SY, Yilmaz FF, Eraç B, Nenni M, Gurer-Orhan H, et al. Formulation and evaluation of fluconazole loaded oral strips for local treatment of oral candidiasis. J Drug Deliv Sci Technol. 2019;49:615–21.
35. Kumria R, Gupta V, Bansal S, Wadhwa J, Nair AB. Oral buccoadhesive films of ondansetron: Development and evaluation. Int J Pharm Investig [Internet]. Medknow Publications & Media Pvt Ltd; 2013;3:112–8. Available from: https://pubmed.ncbi.nlm.nih.gov/24015383.
36. Hoffmann EM, Breitenbach A, Breitkreutz J. Advances in orodispersible films for drug delivery. Expert Opin Drug Deliv. 2011;8:299–316.
37. Saha S, Tomaro-Duchesneau C, Daoud JT, Tabrizian M, Prakash S. Novel probiotic dissolvable carboxymethyl cellulose films as oral health biotherapeutics: In vitro preparation and characterization. Expert Opin Drug Deliv. 2013;10.
38. Pezik E, Gulsun T, Sahin S, Vural İ. Development and characterization of pullulan-based orally disintegrating films containing amlodipine besylate. Eur J Pharm Sci. 2021;156:105597.
39. Hao J, Gao Y, Zhao J, Zhang J, Li Q, Zhao Z, et al. Preparation and Optimization of Resveratrol Nanosuspensions by Antisolvent Precipitation Using Box-Behnken Design. AAPS PharmSciTech. 2014;16:118–28.
40. Arik Kibar EA, Us F. Thermal, mechanical and water adsorption properties of corn starch-carboxymethylcellulose/methylcellulose biodegradable films. J Food Eng. 2013;114:123–31.
41. Ren M, Frimmel FH, Abbt-Braun G. Multi-cycle photocatalytic degradation of bezafibrate by a cast polyvinyl alcohol/titanium dioxide (PVA/TiO2) hybrid film. J Mol Catal A Chem [Internet]. Elsevier B.V.; 2015;400:42–8. Available from: http://dx.doi.org/10.1016/j.molcata.2015.02.004.
42. Zhang Y, Remadevi R, Hinestroza JP, Wang X, Naebe M. Transparent ultraviolet (UV)-shielding films made from waste hemp hurd and polyvinyl alcohol (PVA). Polymers (Basel). 2020;12:1190.
43. Zhang K, Han M, Han L, Ishida H. Resveratrol-based tri-functional benzoxazines: Synthesis, characterization, polymerization, and thermal and flame retardant properties. Eur Polym J [Internet]. Elsevier; 2019;116:526–33. Available from: https://doi.org/10.1016/j.eurpolymj.2019.04.036.
44. Zheng W, Hao Y, Wang D, Huang H, Guo F, Sun Z, et al. Preparation of triamcinolone acetonide-loaded chitosan/fucoidan hydrogel and its potential application as an oral mucosa patch. Carbohydr Polym [Internet]. Elsevier Ltd; 2021;272:118493. Available from: https://doi.org/10.1016/j.carbpol.2021.118493.
45. Tarique J, Sapuan SM, Khalina A. Effect of glycerol plasticizer loading on the physical, mechanical, thermal, and barrier properties of arrowroot (Maranta arundinacea) starch biopolymers. Sci Rep [Internet]. Nature Publishing Group UK; 2021;11:1–17. Available from: https://doi.org/10.1038/s41598-021-93094-y.

46. Dixit RP, Puthli SP. Oral strip technology: Overview and future potential. J Control Release [Internet]. Elsevier B.V.; 2009;139:94–107. Available from: http://dx.doi.org/10.1016/j.jconrel.2009.06.014.
47. Rezaee F, Ganji F. Formulation, Characterization, and Optimization of Captopril Fast-Dissolving Oral Films. AAPS PharmSciTech. 2018;19:2203–12.
48. Mohammadi G, Mirzaeei S, Taghe S, Mohammadi P. Preparation and evaluation of Eudragit® L100 nanoparticles loaded impregnated with kt tromethamine loaded PVA-HEC insertions for ophthalmic drug delivery. Adv Pharm Bull [Internet]. 2019;9:593–600. Available from: https://doi.org/10.15171/apb.2019.068.
49. Nugraheni AD, Purnawati D, Kusumaatmaja A. Physical Evaluation of PVA/Chitosan Film Blends with Glycerine and Calcium Chloride. J Phys Conf Ser. 2018. p. 012052.
50. Pham H, Nguyen QP. Effect of silica nanoparticles on clay swelling and aqueous stability of nanoparticle dispersions. J Nanoparticle Res [Internet]. 2013;16:2137. Available from: https://doi.org/10.1007/s11051-013-2137-9.
51. Takeuchi H, Yamakawa R, Nishimatsu T, Takeuchi Y, Hayakawa K, Maruyama N. Design of rapidly disintegrating drug delivery films for oral doses with hydoxypropyl methylcellulose. J Drug Deliv Sci Technol. 2013;23:471–5.
52. Guidance for Industry Orally Disintegrating Tablets [Internet]. U.S. Dep. Heal. Hum. Serv. Food Drug Adm. Cent. Drug Eval. Res. 2008. Available from: https://www.fda.gov/media/70877/download.
53. Takeuchi Y, Umemura K, Tahara K, Takeuchi H. Formulation design of hydroxypropyl cellulose films for use as orally disintegrating dosage forms. J Drug Deliv Sci Technol [Internet]. Elsevier; 2018;46:93–100. Available from: https://doi.org/10.1016/j.jddst.2018.05.002.
54. Robinson K, Mock C, Liang D. Pre-formulation studies of resveratrol. Drug Dev Ind Pharm. 2015;41:1464–9.
55. Kraemer J, Gajendran J, Guillot A, Schichtel J, Tuereli A. Dissolution testing of orally disintegrating tablets. J Pharm Pharmacol. 2012;64:911–8.
56. Mathematical models of drug release. Strateg to Modify Drug Release from Pharm Syst. 2015. p. 63–86.
57. Paul DR. Elaborations on the Higuchi model for drug delivery. Int J Pharm. 2011;418:13–7.
58. Jain A, Jain SK. In vitro release kinetics model fitting of liposomes: An insight. Chem Phys Lipids. 2016;S0009-3084:30147–5.

Figures

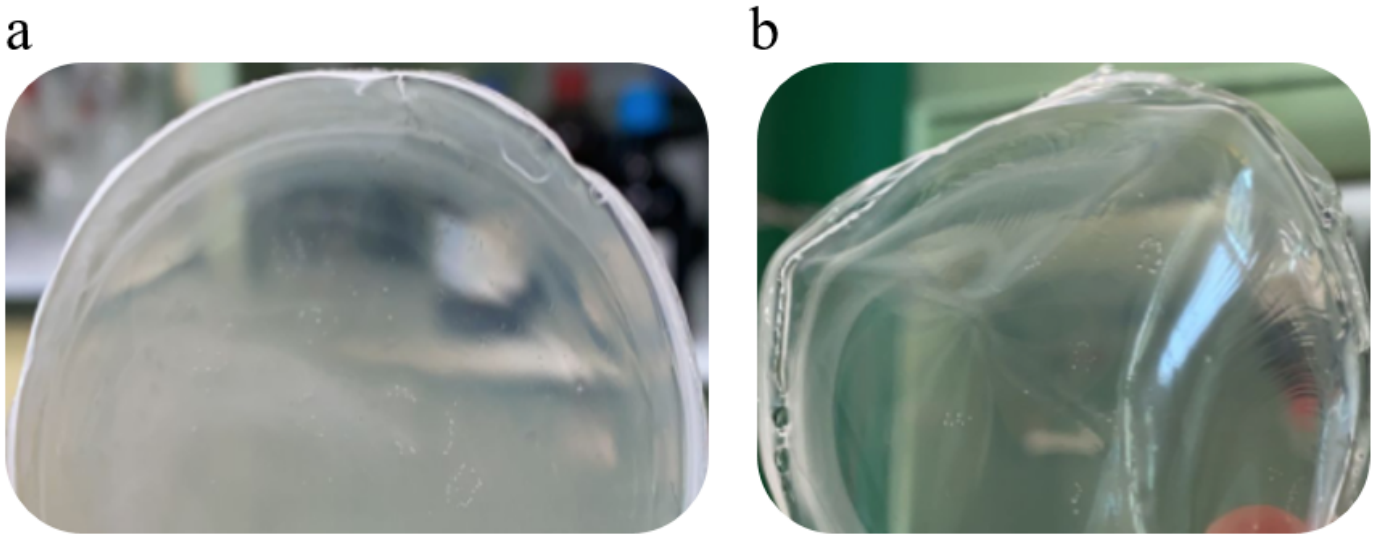

Figure 1

Images of the RES nanocrystal loaded ODFs prepared without (a, F7) or with glycerin (b, F8)

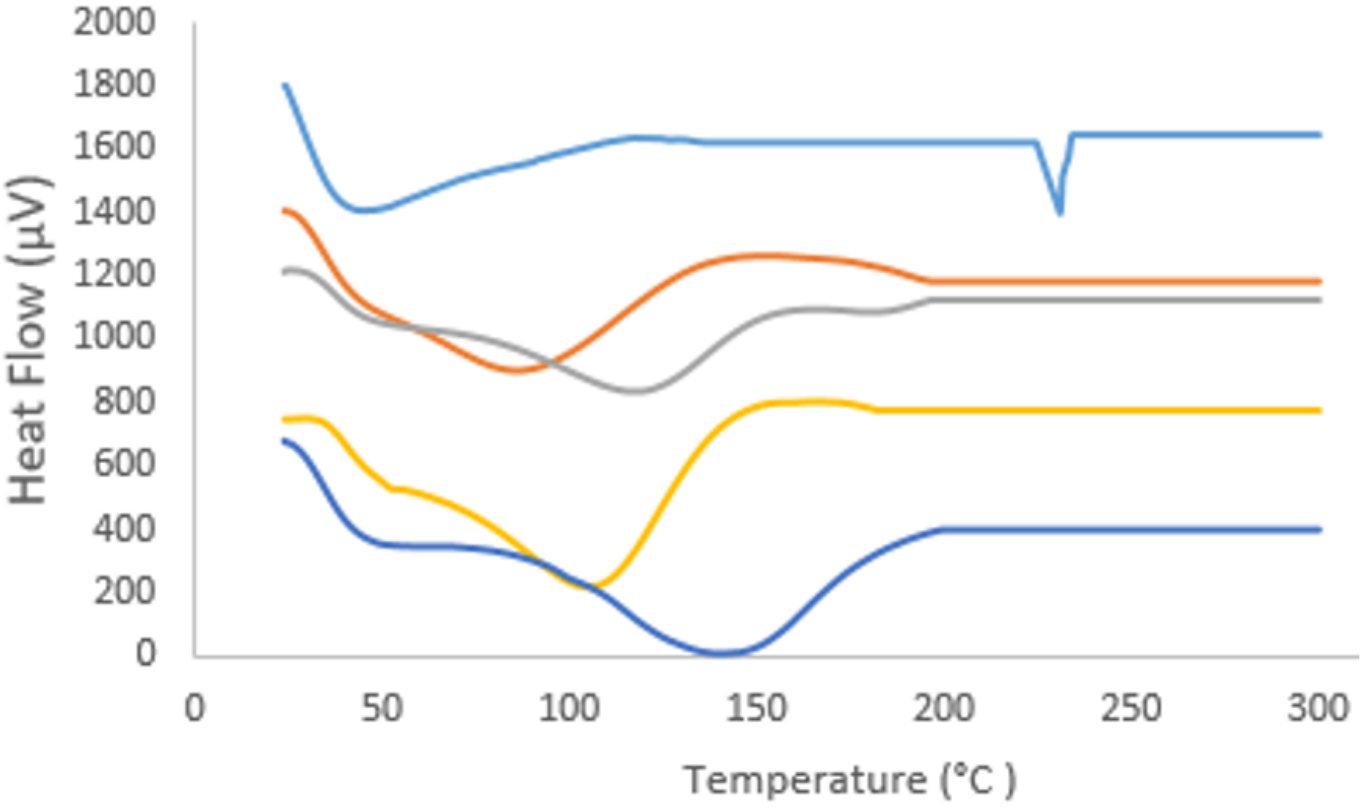

Figure 2

DSC thermograms of the RES nanocrystal loaded ODFs prepared without (F7) or with glycerin (F8) and coarse RES loaded ODFs prepared without (F9) or with (F10) glycerin.

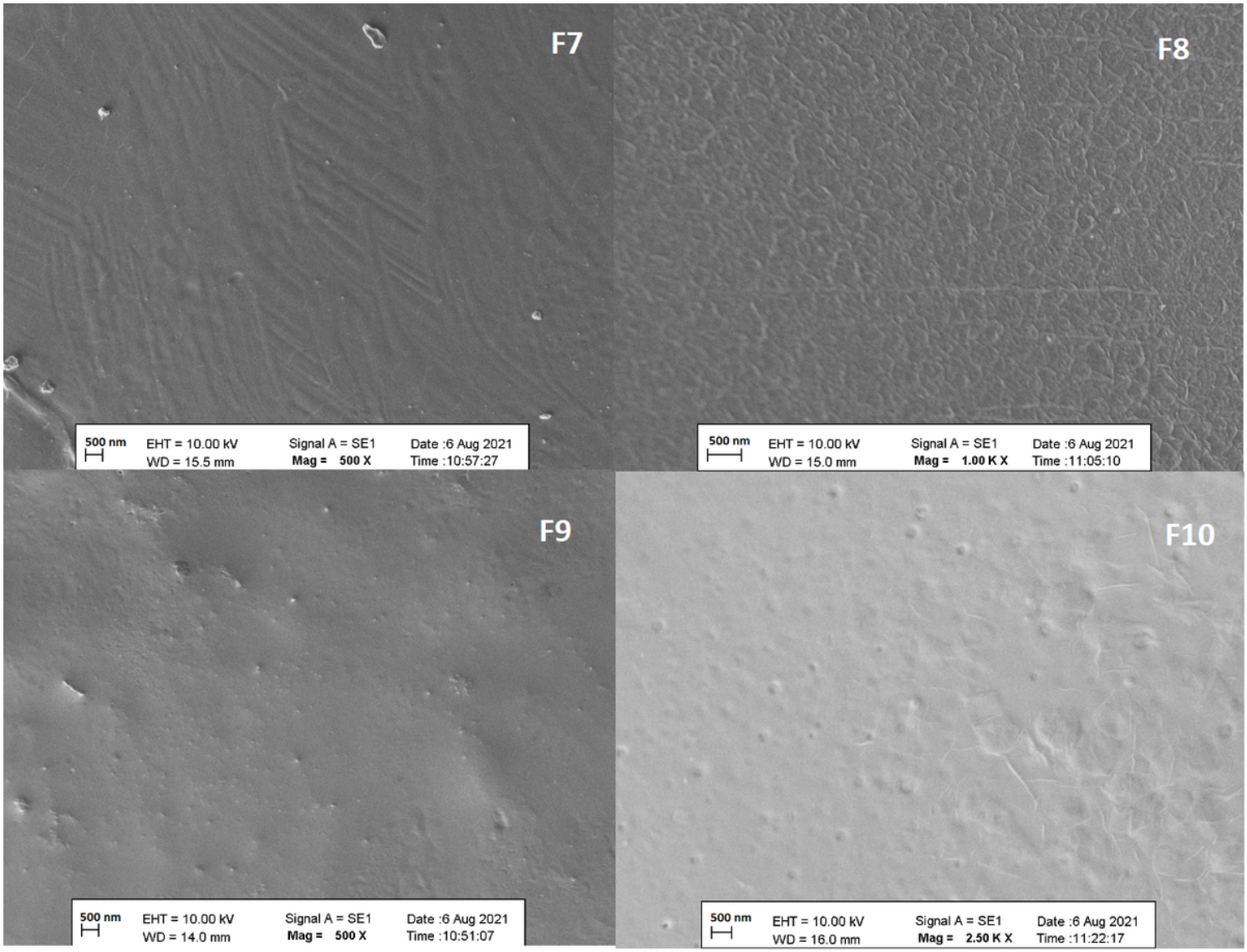

Figure 3

SEM images of the RES nanocrystal loaded ODFs prepared without (F7) or with glycerin (F8) and coarse RES loaded ODFs prepared without (F9) or with (F10) glycerin.

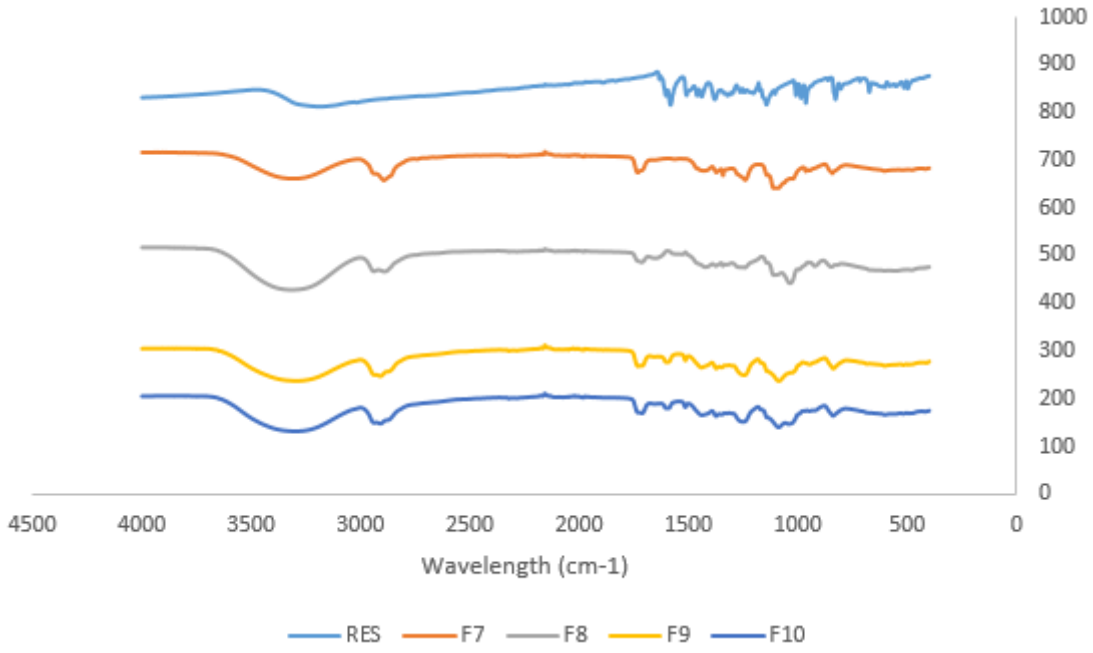

Figure 4

FTIR spectra of the RES nanocrystal films prepared without (F7) or with glycerin (F8) and coarse RES films prepared without (F9) or with (F10) glycerin.

Supplementary Files

This is a list of supplementary files associated with this preprint. Click to download.

- Graphical.png